

FLOW RESEARCH, INC.

A Theory of Hydraulic Rock Cutting

by

Dr. Steven C. Crow

June 1972

Flow Research Report No. 5

A Theory of Hydraulic Rock Cutting

by

Dr. Steven C. Crow †

Flow Research, Inc., Kent, Wa. 98031

Abstract

Water jets having total pressures above 1000 atm are attractive tools for cutting rock. Here a theory is developed to explain the cutting action. The rock is assumed to translate at a speed v under a continuous jet. The problem is to determine the depth h of the resulting slot as a function of feed rate v , diameter d_0 and total pressure P_0 of the jet, and the relevant properties of the rock.

The jet exerts traction against a cutting surface at the leading edge of the slot, and the traction induces continuous fracture. Cavitation tends to sheath the cutting surface in vapor, but curvature of the jet stream causes a high surface pressure, which closes the cavity bubbles and exposes the grains to direct impact from the water. The surface pressure would suffice to keep the grains in place, but permeability allows the water to penetrate beneath the cutting surface and relieve the pressure across the grains.

Permeability gives rise to an intrinsic speed for rock cutting, $c = k\tau_0/\mu_r g$, where k is the permeability, τ_0 the shear strength, and μ_r the coefficient of internal friction of the rock, and g is a typical grain diameter. For Wilkeson sandstone, c is found to be 17.2 in/sec. If the feed rate v is considerably less than c , then the slot depth h is unaffected by permeability and has a value $1.01 d_0 P_0 / \tau_0$ for an optimum angle of jet impingement. The slot depth h decreases as v becomes comparable to c , but the rate of slot-area creation hv rises toward a maximum value $1.47 k d_0 P_0 / \mu_r g$, proportional to permeability but wholly independent of shear strength. At feed rates exceeding $(0.42 P_0 / \tau_0 - 1)c$, the jet stream no longer exerts sufficient traction to fail the rock, and efficient cutting ceases.

The theory is compared to preliminary data spanning a three-decade range of v , and the comparison is highly encouraging.

† Dr. Crow is a Consultant of Flow Research, Inc., presently at the University of California, Los Angeles, California.

Table of Contents

	<u>Page</u>
Abstract	i
Table of Contents	ii
1. Introduction	1
2. Geometry	5
3. Fluid Dynamics	9
4. Shear Stress on the Water Side	12
5. Shear Stress on the Rock Side	17
6. Solution of the Equations	22
7. Comparison with Experiment	24
8. Practical Consequences	29
9. References	31

1. Introduction

This theory was inspired by experiments of J. H. Olsen and B. A. Thomas, who developed a lightweight continuous pressure intensifier for a water jet. The intensifier raises the stagnation pressure of the water up to 20,000 psi, well above the compressive strength of concrete and many rocks. The water jet should serve as a quiet and wear-free cutting tool, a replacement for the jack-hammer.

A developed technology of hydraulic rock cutting would play a major role in the emerging era of rapid transportation. Clearing away existing concrete roads and structures is enormously expensive, and the cost of tunneling depends mainly on the speed with which rock can be penetrated. Despite the economic motivation, little is known about the fundamental mechanics of hydraulic rock cutting, and in fact the action of its traditional competitor, the jack-hammer, is a matter of current research [1].

The English literature on hydraulic rock penetration begins with Farmer and Attewell [2], who released a transient water jet against fixed targets. As a qualitative model of penetration, they imagined the jet impacting as a train of solid projectiles and deforming the rock plastically by momentum transfer. They derived from their experiments an empirical formula for the depth of penetration, but the formula was not consistent with the momentum-transfer argument.

Farmer and Attewell were followed by Leach and Walker [3], who were mainly concerned with the effect of nozzle shape on the coherence of the jet. They performed limited experiments on rock penetration by ejecting 10 cm^3 of water under pressures ranging from 1000 to 6000 atm. They discovered that no penetration occurs if the total pressure P_o of the jet stream lies below a critical value P_c , which depends on the type of rock. The depth of penetration appeared to be proportional to $(P_o - P_c)$ above the critical pressure, the constant of proportionality depending again on the type of rock. It is worth noting that a high constant of proportionality did not imply a low value of P_c , which means that initial fracture and final depth of penetration are controlled by different mechanisms. Brook and Summers [4] followed with an experimental study of penetration into static targets as a function of standoff distance, driving pressure P_o , and duration of the jet stream. The penetration depth was proportional to P_o , rising rapidly in the first few milliseconds of jet impingement, then much more gradually with further elapse of time. The critical pressure P_c was too low for observation,

presumably because the sandstone targets were too soft. Recently Powell and Simpson [5] attempted to calculate P_c on the basis of elasticity theory and a fracture criterion. The results proved to be higher than those reported in [3], and Powell and Simpson concluded that "the rock cutting action of a water jet cannot be explained entirely in terms of mechanical fracture due to the stress field induced internally in the rock by impact of the jet."

The English work produced useful correlations but no explanation of the mechanics of hydraulic rock cutting. The explanation had to go beyond a simple fracture criterion, to the interplay between the fluid mechanics of the jet stream and the solid mechanics of the rock.

One reason no explanation was forthcoming may be that penetration of a static target is a difficult conceptual problem. The hole deepens with time, and the interface between water and rock is nonsteady. Olsen and Thomas's continuous-flow pressure intensifier lends itself to the alternative steady-state experiment illustrated in Fig. 1. The jet emerges with diameter d_o and steady total pressure P_o , and the rock feeds under the jet stream at a constant speed v . However complicated the mechanics of cutting may be, the cutting interface is steady in coordinates fixed with respect to the jet, and the cut attains some definite terminal depth h . The problem is to determine h as a function of P_o , d_o , v , and whatever material properties may be pertinent.

Soviet workers developed continuous-flow pressure intensifiers early and have published experimental data on h . Zelenin, Vesselov, and Koniashin [6] cut three kinds of stone — granite, limestone, and marble — at pressures P_o up to 2000 atm. They found that h is directly proportional to $(P_o - P_c)$ and inversely proportional to a measure of rock hardness, which here will be taken as the shear strength τ_o . The critical pressure P_c was found to increase with feed rate v . For each P_o , cutting would cease at a sufficiently high value of v , and the only effect of the jet would be sporadic pitting. Perhaps the most interesting finding was that h is independent of v for feed rates up to about 10 in/sec and thereafter decreases gradually with v until cutting ceases altogether. The results of [6] can be summarized by the formula

$$h = d_o \frac{(P_o - P_c)}{\tau_o} F(v) \quad , \quad (1)$$

where P_c increases with v , and $F(v)$ is constant at low v and decreases at higher v . Zelenin, Vesselov, and Koniashin assert that $F(v)$ falls as $v^{-0.33}$ in the feed-rate interval 20-70 in/sec, though no simple power law will suffice for all v .

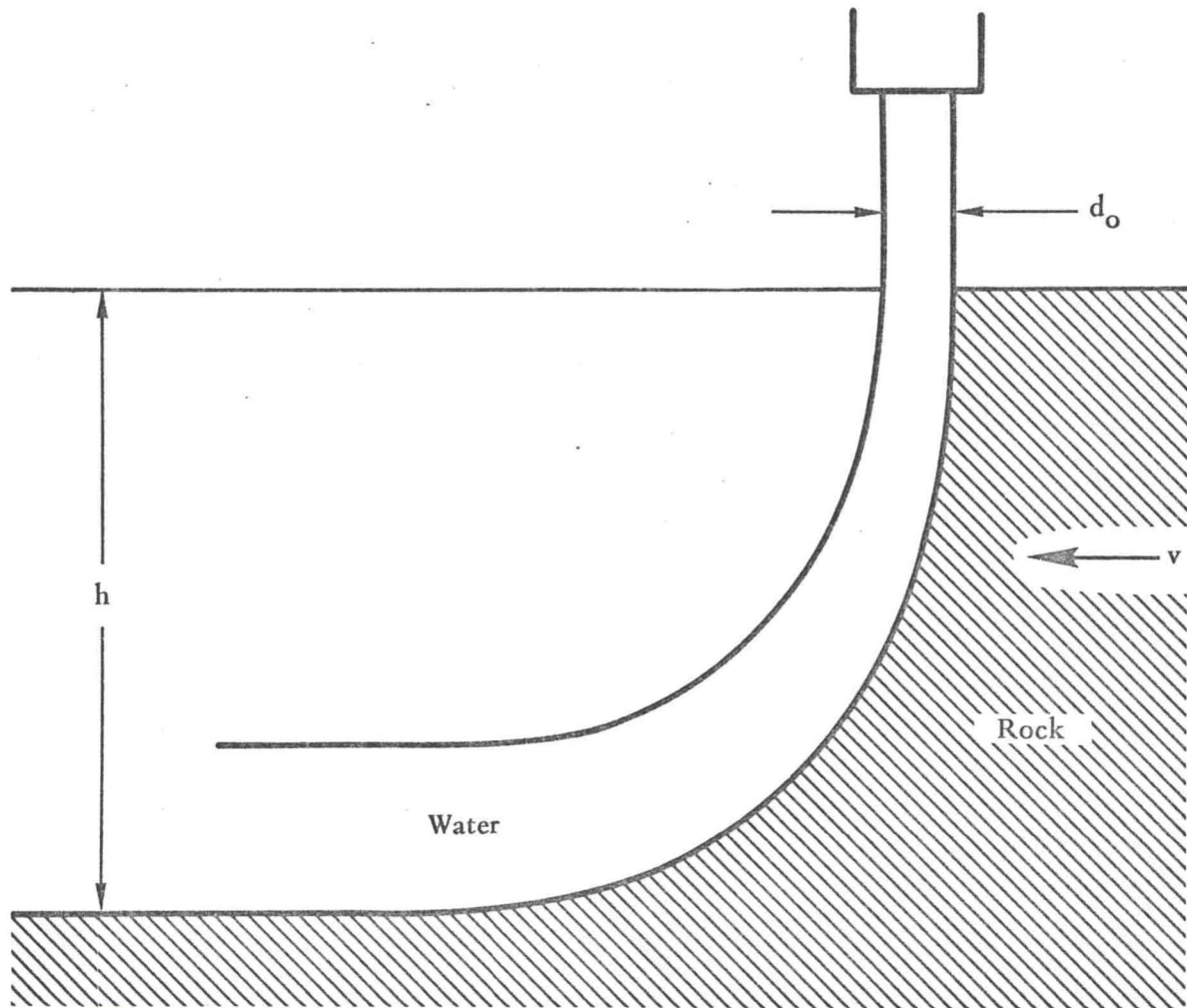


Figure 1. Cutting by a steady high-speed water jet.

Notice from equation (1) that $F(v)$ is dimensionless. There must be a speed intrinsic to the cutting process upon which v can scale, an intrinsic speed c of order 10-100 in/sec. The speed of a water jet at 1000 atm is about 1500 ft/sec, and the speed of shear waves in rock is 5000 ft/sec or better. Both are much too high to serve as the intrinsic speed for rock cutting.

The theory of hydraulic rock cutting must admit a surprising variety of phenomena, including cavitation, brittle fracture, and permeability. A rectilinear water flow passing at high speed over a granular interface would exert little shear stress, because the interface would be in a state of almost complete cavitation. The jet curves against the cutting surface as shown in Fig. 1, however, and the curvature induces a high surface pressure, which closes cavity bubbles and exposes the grains to direct impact from the water. The surface pressure would keep the grains in their sockets, were it not for the finite permeability of the rock. Permeability gives rise to a pore pressure beneath the cutting surface, which relieves the normal force on the grains and allows them to be shorn away. The intrinsic speed c is found to be $k\tau_o/\mu_r g$, where k is the permeability of the rock, μ_r is its coefficient of internal friction, and g is a typical grain diameter.

A mathematical theory based on those phenomena is constructed in the next five sections and compared to measurements of Olsen and Thomas in Section 7. The data are not exhaustive but do cover a three-decade range of v . The data serve mainly to enhance the plausibility of the theory and to fix a universal constant, the coefficient μ_w of Coulomb friction between water and rock under cavitational conditions.

2. Geometry

Olsen and Thomas have observed that their water jet leaves a clean cut in sandstone, more suggestive of erosion than of gross internal failure. One can therefore make some expedient assumptions about the geometry of the cut without straying far from reality. The idealized cut is shown in Fig. 2. The jet is presumed to enter with a square cross-section of width and depth d_0 , and to leave behind a uniform slot of width d_0 . Cutting thus takes place entirely on the forward face of the jet, where the surface pressure due to streamline curvature is greatest. Friction against the cutting surface decelerates the jet, and the stream must deepen to accommodate the constant volume flow of water. The local depth d increases station-by-station downstream.

Hopefully the reader will not be put off by the geometrical assumptions, which may appear sweeping. The assumption of a square jet may seem strange, especially since d_0 is identified later with nozzle diameter, and the cut is never quite so narrow as the nozzle diameter itself. The purpose of this paper is to frame the physics of hydraulic rock cutting in a geometry that admits simple analysis. The solution for h will contain the empirical universal constant μ_w , which can absorb minor geometrical deficiencies.

Figure 3 illustrates the geometrical properties of the cutting surface. The surface follows the curve $y(x)$, where the ordinate y increases downward into the stone, and the abscissa x increases backward along the cut. The origin of the coordinate system is the point where the jet first impacts the stone. The arc-length s specifies location along the cutting surface, and θ is the local angle of the cut with respect to the horizontal. Note that the jet can enter at an angle θ_0 different than 90° and is so illustrated. Experiments have been carried out to date under conditions of normal impingement, $\theta_0 = 90^\circ$, but the theory indicates that impingement angles θ_0 greater than 90° will produce deeper cuts (cf. Section 8).

The quantity connecting geometry to dynamics is the local radius of curvature of the cutting surface,

$$R = - \frac{ds}{d\theta} . \quad (2)$$

Now x and y can be expressed in terms of R as follows. Note that

$$\frac{dy}{ds} = \frac{dy}{d\theta} \frac{d\theta}{ds} = \sin \theta ,$$

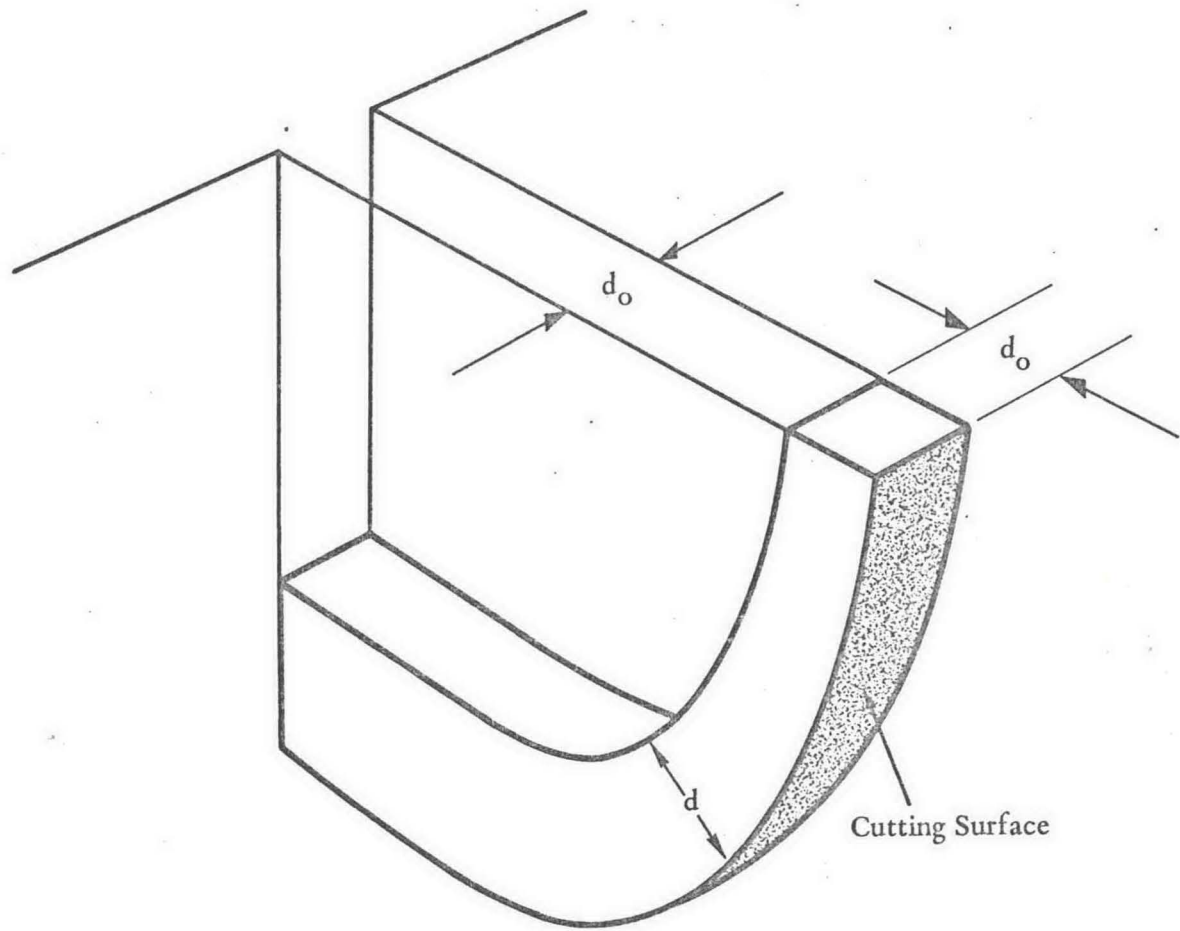


Figure 2. Geometry of the idealized cut.

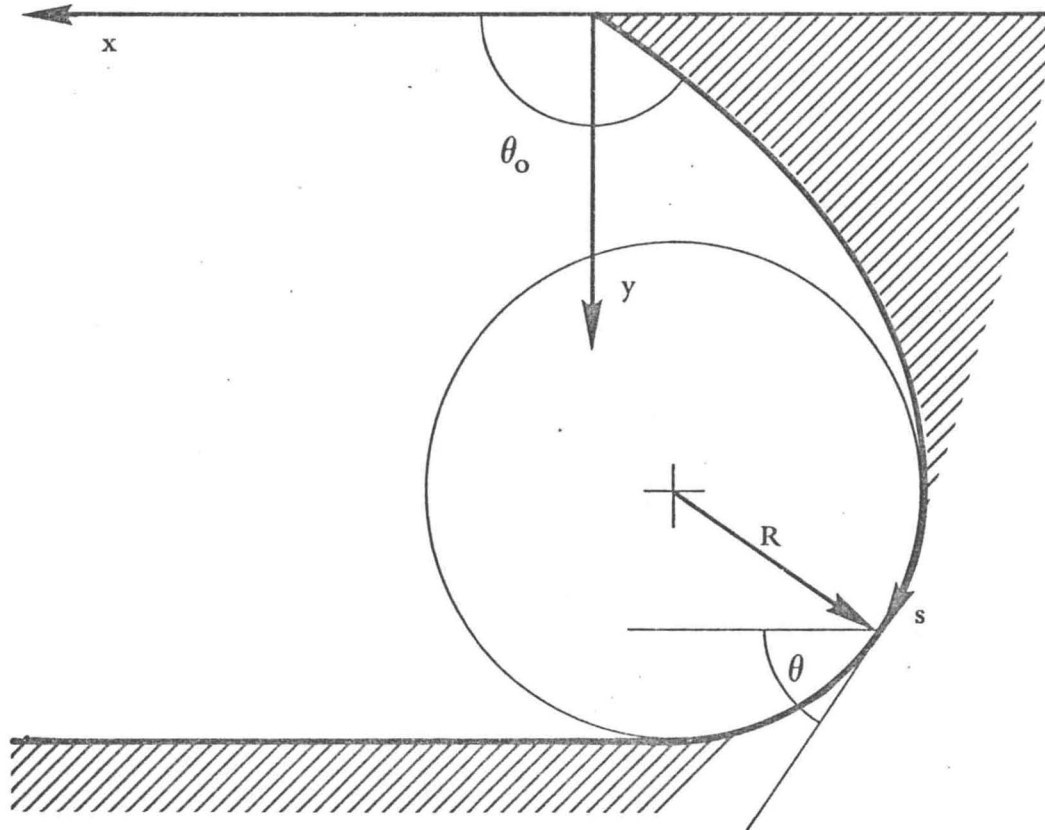


Figure 3. Geometry of the cutting surface. The jet enters with a positive rake (cf. Section 8).

and by equation (2), therefore,

$$\frac{dy}{d\theta} = -R \sin \theta .$$

In the same fashion,

$$\frac{dx}{d\theta} = -R \cos \theta ,$$

and the final expressions for x and y are obtained by integration:

$$\left. \begin{aligned} x(\theta_s) &= \int_{\theta_s}^{\theta_0} R(\theta) \cos \theta \, d\theta , \\ y(\theta_s) &= \int_{\theta_s}^{\theta_0} R(\theta) \sin \theta \, d\theta . \end{aligned} \right\} \quad (3)$$

The function $y(x)$ is thus available in parametric form, the parameter being the cutting angle θ_s at the endpoint of the integration.

The impingement angle θ_0 can lie between 0° and 180° . The local angle θ_s falls to 0° at the deepest point of the cut. θ_s cannot fall below 0° , because negative θ_s would mean the rock somehow were reconsolidating and filling up the cut. It follows that the depth h of the cut is given by the formula

$$h = \int_0^{\theta_0} R(\theta) \sin \theta \, d\theta , \quad (4)$$

which is the main result of this section. The task remains for dynamics to determine the local radius of curvature R as a function of angle θ .

One further geometrical assumption will be made to simplify the fluid dynamics, namely that the depth d of the jet stream is everywhere small compared with the radius of curvature R :

$$d \ll R \quad \text{or} \quad d_0 \ll h . \quad (5)$$

The two inequalities are essentially equivalent. The theory is tailored to deep cuts, but the predictions agree with data measured by Olsen and Thomas down to $h/d_0 \approx 1$. Shallower cuts give way to pitting and spalling, so the theory seems valid over the whole regime where the notion of "cutting" itself is warranted.

3. Fluid Dynamics

The equations of motion are best written in the form of integrals through the depth of the curved jet. The variable of integration is the normal coordinate n , perpendicular to the streamwise coordinate s as shown in Fig. 4. The density of the water is ρ , constant throughout the flow under conditions attainable by Olsen and Thomas's rock cutter. The speed of the water is u and the pressure is p at the location (s,n) . Along the interface (s,d) between air and water, p must equal the atmospheric pressure p_a . Streamline curvature raises p to some higher value p_s at the cutting surface $(s,0)$. The water speed u is uniform across the jet at $s = 0$ and has a value u_o related to the stagnation pressure P_o in the pressure intensifier by the Bernoulli equation:

$$P_o - p_a = \frac{1}{2} \rho u_o^2 . \quad (6)$$

The width of the jet is constant by assumption, so the equation of volume conservation takes the form

$$\int_0^d u \, dn = u_o d_o . \quad (7)$$

Equation (7) could be used to calculate the local depth d of the stream, but (7) is not needed to determine h in the present theory and will not be seen again.

Conservation of momentum normal to the streamlines results in a pressure balance:

$$P_s - p_a = \frac{1}{R} \int_0^d \rho u^2 \, dn . \quad (8)$$

It is at this stage that approximation (5) first enters the analysis. If the jet were not thin compared with its radius of curvature, then the variation of R from one streamline to the next would have to be taken into account, and R would have to be included under the integral in equation (8). Under approximation (5), all streamlines share a common radius of curvature R at station s .

It is worthwhile to examine the magnitude of the hydrodynamic pressure p_s against the cutting surface. Suppose P_o is 1000 atm, that is $P_o = 1000 p_a$. The momentum flux ρu^2 is of order ρu_o^2 , which is about $2 P_o$ according to (6). Thus $\rho u^2 \approx 2000 p_a$. The ratio d/R is assumed small, say $d/R = 0.1$, so $p_s \approx 200 p_a$.

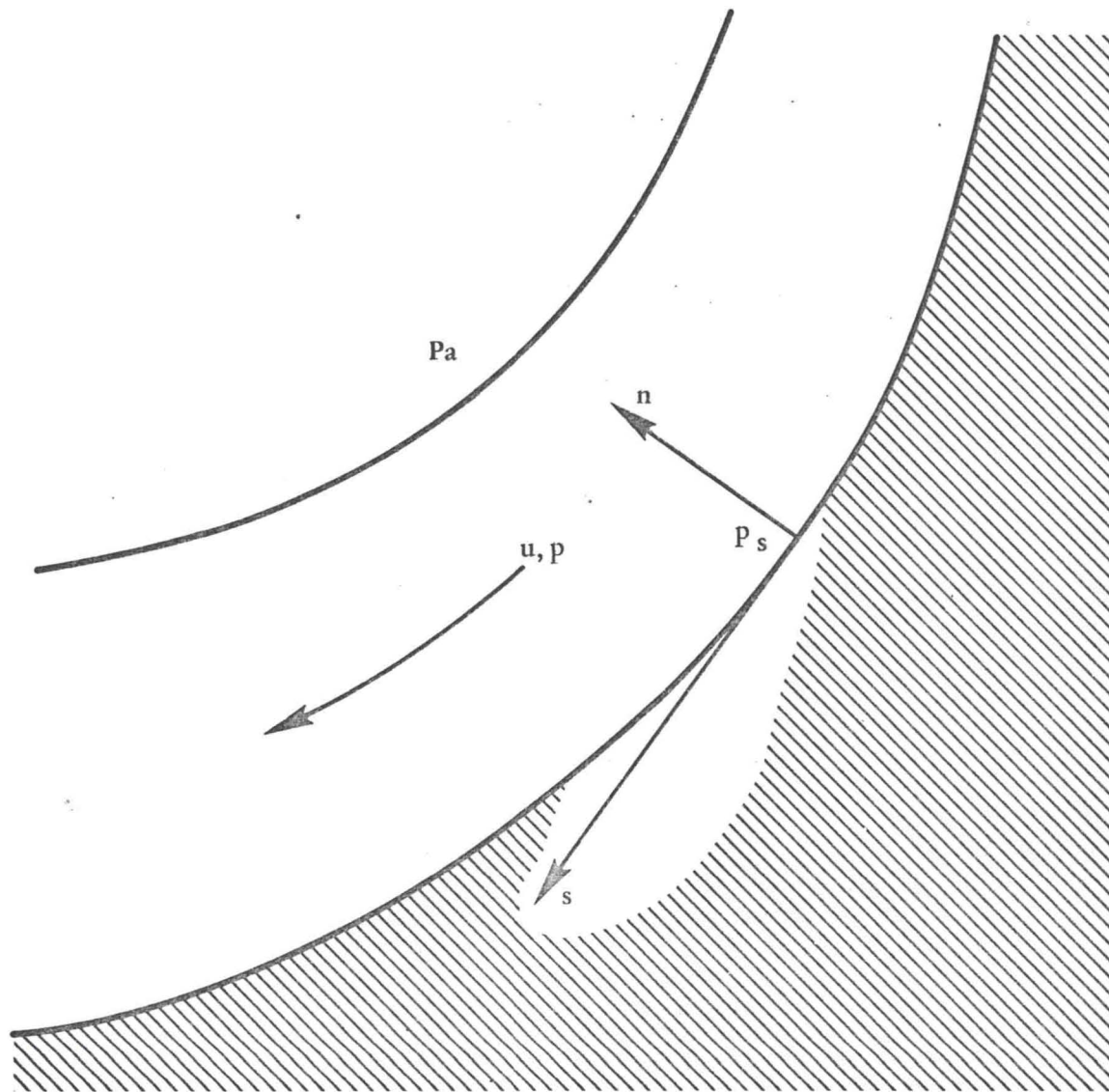


Figure 4. Quantities entering the equations for volume and momentum conservation.

The surface pressure p_s is therefore enormous by ordinary standards but is a small fraction of the total pressure P_o of the water jet.

The final equation of motion relates the decay of streamwise momentum flux ρu^2 to the shear stress τ on the cutting surface:

$$\frac{d}{ds} \int_0^d \rho u^2 dn = -\tau. \quad (9)$$

Strictly speaking, the integral should contain pressure terms as well, but equation (8) implies that the pressure p is of order $(d/R)\rho u^2$, which is negligible compared with ρu^2 under approximation (5). The neglect of pressure in the streamwise-momentum equation (9) is analogous to the boundary layer approximation in classical fluid dynamics.

Equation (9) can be transformed into a less familiar form, but one better suited to later calculations. Note first that the derivative d/ds with respect to arc-length can be written as $(-1/R) d/d\theta$ by virtue of equation (2). The momentum integral appearing in (9), moreover, is exactly the same as the integral in (8), regardless of how $u(s,n)$ may vary with n . The streamwise-momentum equation thus takes the form

$$\frac{d}{d\theta} [R(p_s - p_a)] = R\tau, \quad (10)$$

which will become a differential equation for $R(\theta)$ under appropriate assumptions about τ .

4. Shear Stress on the Water Side

The interfacial shear stress τ is caused by the drag of water upon grains protruding from the cutting surface. To construct a model of τ , one must understand the general nature of the flow around a grain. The typical grain will be treated as a rough sphere, having a diameter g small compared with the stream depth d so that the grain participates in the hydrodynamic environment of the cutting surface. Consider, as a specific instance, the Olsen and Thomas experiment described in Section 7. P_0 was 17,000 psi, and therefore $u_0 = 1600$ ft/sec according to the Bernoulli equation (6). The grain diameter g was about 0.005 inch, reasonably small compared with the 0.030-inch diameter of the nozzle.

The speed a of sound in water is 4800 ft/sec, so the Mach number u/a of the flow around a grain was modest,

$$\frac{u}{a} \approx \frac{1600}{4800} \approx 0.3 ,$$

small enough that the flow could be considered incompressible if it were steady. Grain removal could result in nonsteady compressibility effects, called "water hammer" in hydraulics, and water hammer has been advanced as a mechanism for hydraulic rock cutting [7]. But water hammer would be important only if a typical grain-removal time t were so short that the Helmholtz number g/at were of order unity. It is hard to imagine t being shorter than g/u , the time required for a grain to traverse its own diameter while moving with the flow, so the Helmholtz and Mach numbers are of the same order u/a . Neither steady nor non-steady compressibility effects should be important. Likewise with viscous effects, because the Reynolds number of the flow around the grain is high,

$$\frac{\rho u g}{\eta} \approx 58,000 ,$$

where η is the viscosity of the water.

The essential phenomenon governing the shear stress is cavitation. The cavitation number at the cutting surface is

$$\frac{p_s - p_v}{\frac{1}{2} \rho u^2} ,$$

where p_v is the vapor pressure of the water, and ρu^2 can be taken as the average

of the momentum flux through the jet. It follows from equation (8) that

$$\frac{p_s - p_v}{\frac{1}{2} \rho u^2} \approx 2 \frac{d}{R},$$

where p_a and p_v have been regarded as negligible compared with p_s . The cavitation number is therefore small under the basic approximation (5) of this theory, and a small cavitation number means that cavity bubbles trail behind the grains. The cutting surface appears to the water flow as an intricate patchwork of grains and vapor cavities. As the radius of curvature R increases, the level of cavitation increases, and the water loses contact with the grains. As the radius of curvature decreases, the surface pressure p_s increases and collapses the cavity bubbles, thereby exposing more grains to direct impact of the water. The interfacial shear stress should therefore be written as

$$\tau = \frac{1}{2} \rho u^2 c_f \left(\frac{p_s - p_v}{\frac{1}{2} \rho u^2} \right), \quad (11)$$

where the skin-friction coefficient c_f is some increasing function of the cavitation number.

Further progress requires that (11) be reduced to an explicit form. Consider the model sketched in Fig. 5. One grain taking the full impact of the water shields some of its neighbors downstream. If ℓ is the streamwise separation between fully exposed grains, then each exposure blanks an area $g\ell$. If f is the drag of an exposed grain, then

$$\tau = \frac{f}{g\ell}.$$

But

$$f = C_D (\pi g^2 / 8) \frac{1}{2} \rho u^2,$$

where C_D is the drag coefficient of a grain, and $(\pi g^2 / 8)$ is half its cross-sectional area, presumed to be the amount of area exposed above the rocky matrix. The separation ℓ is the sum of the grain diameter and the length of the cavity bubble. To a reasonable approximation, the length of a cavity bubble is found to vary inversely as the cavitation number [8], so one can write

$$\ell = g + gB \left(\frac{\frac{1}{2} \rho u^2}{p_s - p_v} \right).$$

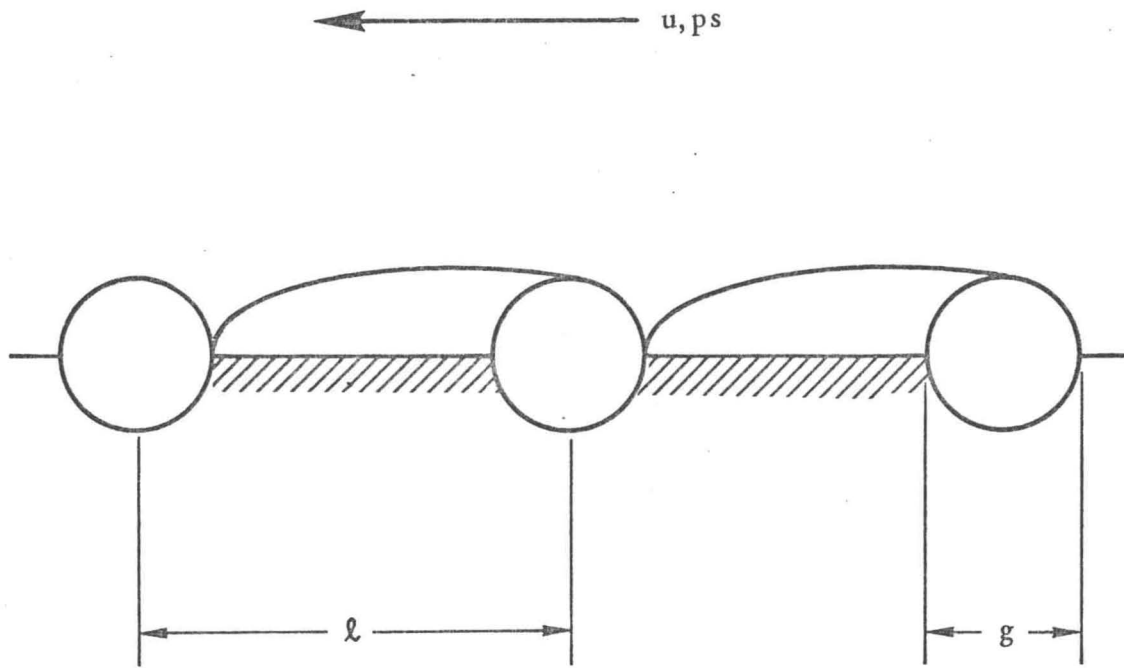


Figure 5. Cavitation model. Ellipsoidal cavity bubbles trail behind round grains. The grains are small enough that the ambient pressure several grain diameters above them is the surface pressure p_s .

Thus

$$\begin{aligned} \tau &= \frac{\frac{\pi}{8} C_D \frac{1}{2} \rho u^2}{1 + B \left(\frac{\frac{1}{2} \rho u^2}{p_s - p_v} \right)} \\ &= \frac{\mu_w (p_s - p_v)}{1 + \left(\frac{p_s - p_v}{\frac{B}{2} \rho u^2} \right)}, \end{aligned} \quad (12)$$

where μ_w is a dimensionless coefficient involving B and C_D :

$$\mu_w = \frac{\pi C_D}{8B}. \quad (13)$$

The model equation (12) is consistent, of course, with the more general expression (11).

The constant B is approximately 0.5 according to [8], so the bracketed quantity in the denominator of (12) is about 4.0 d/R , generally rather small compared with unity, and very much smaller than unity if the inequalities (5) are taken seriously. A remarkably simple friction law follows,

$$\tau = \mu_w (p_s - p_v) \quad (14)$$

within the domain of validity for this theory. The water exerts Coulomb friction upon the rock, a friction proportional to normal pressure but independent of flow speed. The absence of u in (14) may seem paradoxical, since the surface stress τ is due entirely to ram impact of water against the grains. Clearly τ should equal zero when u does. The original friction law (12) involves u and implies that τ and u go to zero simultaneously. Under conditions of strong cavitation, however, an increase in u decreases the contact between water and grains, and the decreased contact exactly compensates the increased dynamic pressure.

Equation (13) permits a rough estimate of μ_w . The constant B is about 0.5 as mentioned before, and C_D is about 0.4 for cavitation flow around a sphere and 0.8 for a flat disc [9]. The drag of an irregular grain should lie somewhere between that of a sphere and a disc, so the coefficient of Coulomb friction is

likely to lie in the interval

$$\mu_w = 0.3 \text{ to } 0.6 . \quad (15)$$

The exact value must be determined experimentally.

5. Shear Stress on the Rock Side

In order to pace the jet, the cutting surface must be in a continuous state of incipient failure. The purpose of this section is to set forth a failure criterion to complement the friction law (14) and close the problem.

An obvious possibility is that the surface fractures when the shear stress reaches some definite value

$$\tau = \tau_0, \quad (16)$$

where τ_0 is the force required to shear off a grain, divided by a typical grain area. Equation (16), however, is overly simple. The normal force on a grain tends to keep it in place, so the right-hand side of (16) must be augmented by a term proportional to normal pressure:

$$\tau = \tau_0 + \mu_r p_s. \quad (17)$$

The failure criterion (17) is due to Coulomb and is discussed in great depth by Jaeger and Cook [10]. μ_r is the coefficient of internal friction for the rock. Generally $\mu_r \approx 1.0$.

Equations (14) and (17) are similar in structure, and a closer inspection reveals that the similarity means trouble. The coefficient μ_w of Coulomb friction between water and rock should not be more than 0.6 according to (15), and certainly μ_w should be less than the coefficient μ_r of friction internal to the rock itself. The shear stress required for fracture according to (17) appears to exceed the stress available from the flow according to (14). A jet should be quite incapable of cutting rock!

The resolution of the dilemma lies in the finite permeability of the rock. The high surface pressure p_s forces water through the pores of the cutting surface, creating a precursor of saturated rock as shown in Fig. 6. The pore pressure p within the saturated region ranges from p_s at the cutting surface CS down to p_a at the interface WD between wet and dry rock. The pore pressure relieves the internal friction and results in a failure criterion

$$\tau = \tau_0 + \mu_r (p_s - p), \quad (18)$$

also discussed at length by Jaeger and Cook.

The pressure difference ($p_s - p$) just beneath the cutting surface can be found by applying Darcy's law for the flow of fluid through a porous medium:

$$\underline{v} - \underline{u} = k \nabla p . \quad (19)$$

Darcy's law has been written in a special form to accommodate the motion of the rock in the present coordinates. k is the permeability of the rock, \underline{v} is the vector velocity, and \underline{u} is the volume flux of fluid through the pores. \underline{u} can be understood by imagining a small pillbox cut into the rock broadside to the flow. \underline{u} would then be the velocity of the fluid through the pillbox.

Now consider the saturated region CSDW in Fig. 6, and assume that the sides CW and SD have some depth δ small compared with the other dimensions like d (the proof that δ is small will be given shortly). Since WD is an air-water interface, no flow can take place across it in the coordinates chosen. Whatever flow takes place through the narrow sides CW and SD is negligible, so flow into the cutting surface CS must be essentially zero to conserve water volume. The same argument applies to any surface parallel to CS, and the component of \underline{u} normal to the cutting surface is therefore zero throughout the saturated region CSDW. If the rock feeds under the jet at a speed v , then the normal component of rock velocity is $v \sin \theta$ as seen in Fig. 6. The normal component of Darcy's law (19) is therefore

$$v \sin \theta = k \frac{\partial p}{\partial n} .$$

The pore pressure beneath the cutting surface follows by integration:

$$p_s - p = \begin{cases} \frac{|n| v \sin \theta}{k} , & |n| < \delta ; \\ p_s - p_a , & |n| > \delta . \end{cases} \quad (20)$$

The absolute value $|n|$ is used to avoid minus signs, since the normal coordinate n is negative on the rock side of the cutting surface.

The criterion for failure of the cutting surface is based on a hypothesis fundamental to this theory: the rock is in a continuous state of incipient fracture one grain diameter g beneath the cutting surface. Setting $|n| = g$ and combining (18) and (20), one arrives at the following expression for the shear stress on the rock side of the cutting surface:

$$\tau = \tau_o + \mu_r \frac{gv}{k} \sin \theta . \quad (21)$$

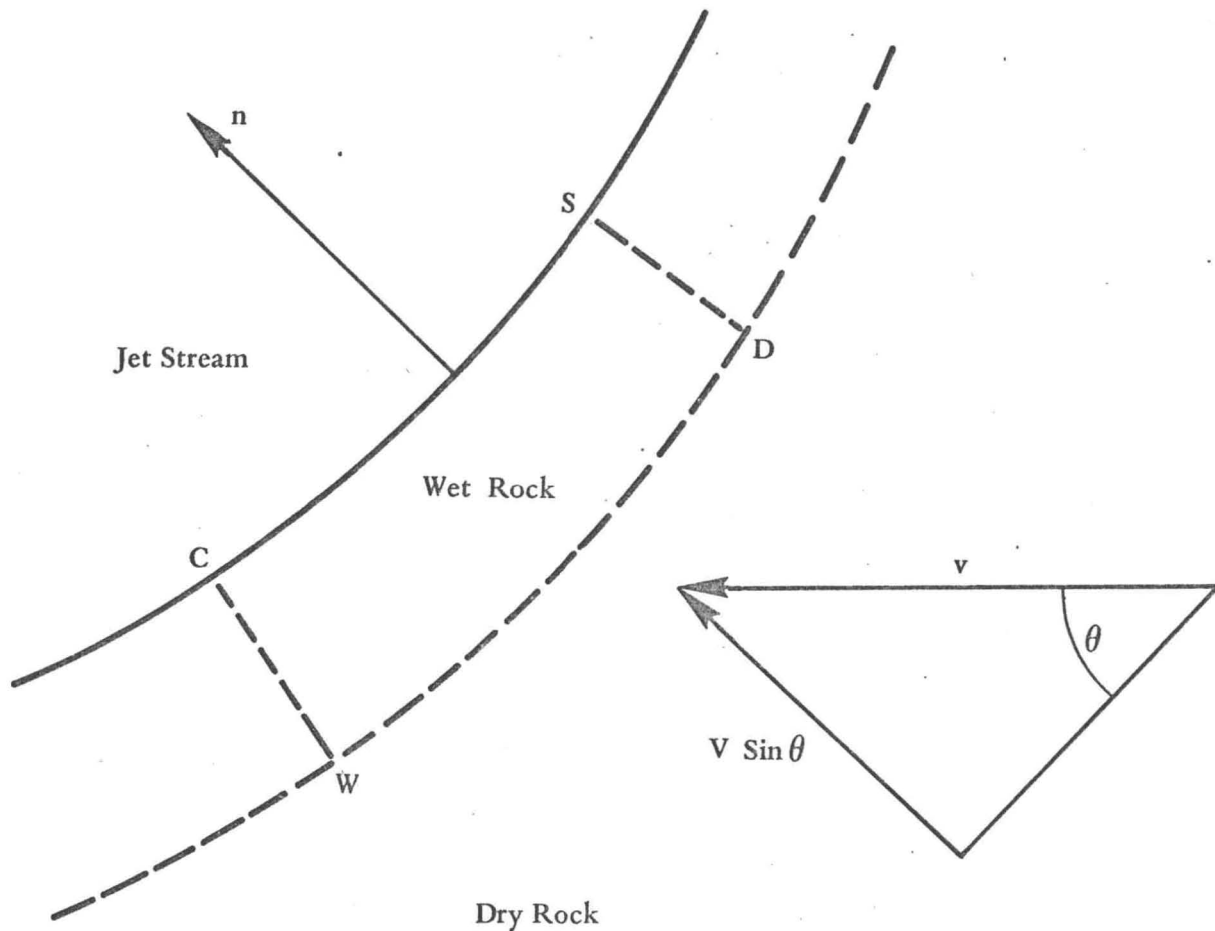


Figure 6. Permeability model. A front WD between wet and dry rock precedes the cutting surface CS.

Implicit in (21) is an intrinsic speed for rock cutting,

$$c = \frac{k\tau_o}{\mu_r g} , \quad (22)$$

which depends on all four properties of the rock but is independent of the jet. The failure criterion (21) can be rewritten in terms of the intrinsic speed as follows:

$$\tau = \tau_o \left(1 + \frac{v}{c} \sin \theta\right) . \quad (23)$$

When (23) is satisfied, the surface layer of grains is always on the verge of being shorn away.

It is now possible to show a posteriori that the thickness δ of the saturated front is indeed small. Since the two forms of (20) must be equal at $|n| = \delta$,

$$\delta = \frac{k(p_s - p_a)}{v \sin \theta} = \mu_r g \frac{p_s - p_a}{\tau - \tau_o} ,$$

where the second equality follows from (21). But (14) must be satisfied simultaneously, so

$$\delta = g \frac{\mu_r}{\mu_w} \frac{\tau}{\tau - \tau_o} .$$

δ is larger than g provided $\mu_r > \mu_w$, but not much larger unless τ is very nearly equal to τ_o , in which case permeability is unimportant anyway. Thus δ is small in a fine-grained rock.

Equations (23) and (14) give rise to a compatibility condition between the fluid and solid mechanics:

$$\mu_w (p_s - p_v) = \tau_o \left(1 + \frac{v}{c} \sin \theta\right) . \quad (24)$$

It is interesting to inquire whether there are circumstances under which (24) cannot be satisfied. Consider the location $\sin \theta = 1$, where the right-hand side of (24) is maximum, and imagine v increasing indefinitely. Equation (8) suggests that p_s can also rise to any level if R becomes small enough. But equation (8) breaks down when $R \sim d$, and p_s cannot rise above the stagnation pressure P_o of the jet. If P_o lies below a critical value P_c given by

$$P_c = \frac{\tau_o}{\mu_w} (1 + v/c) , \quad (25)$$

then the compatibility condition (24) cannot be satisfied, and cutting should not take place. Equation (25) agrees qualitatively with the observations of Zelenin, Vesselov, and Koniashin discussed in Section 1. P_c has some finite value at $v = 0$ and rises linearly with v . Cutting ceases at sufficiently high v for any fixed P_o .

6. Solution of the Equations

Solution of the equations is a simple matter under the present physical assumptions. One begins by deriving an equation for the radius of curvature from the fluid mechanics of Sections 3 and 4. The friction law (14) can be used to eliminate stress from the momentum equation (10), with the result that

$$\frac{1}{\mu_w} \frac{d}{d\theta} R(p_s - p_a) = R(p_s - p_a) + R(p_a - p_v) .$$

Both p_a and p_v are negligible for rock-cutting applications, so the second term on the right-hand side can be dropped. The rest of the equation is immediately integrable:

$$R(p_s - p_a) = R_o(p_s - p_a)_o e^{\mu_w(\theta - \theta_o)} , \quad (26)$$

where the subscript o refers to conditions at the beginning of the cut. From equation (8),

$$R_o(p_s - p_a)_o = \rho u_o^2 d_o ,$$

since the jet is initially uniform and has a speed u_o . Then from the Bernoulli equation (6),

$$R_o(p_s - p_a)_o = 2(P_o - p_a) d_o ,$$

and equation (26) becomes

$$R(p_s - p_a) = 2(P_o - p_a) d_o e^{\mu_w(\theta - \theta_o)} .$$

A second application of (14) eliminates $(p_s - p_a)$ in favor of τ :

$$(p_s - p_a) = \tau/\mu_w - (p_a - p_v) .$$

Thus

$$R = 2 \mu_w \frac{d_o P_o}{\tau} e^{\mu_w(\theta - \theta_o)} , \quad (27)$$

where p_a has been neglected compared with P_o and $(p_a - p_v)$ compared with τ/μ_w , in conformity with the approximation that led to (26). Equation (27) is the final result of the fluid-mechanical arguments.

Combining equation (27) with the solid mechanics of (23) and the geometry of (4), one arrives at the desired formula for the slot depth h :

$$h = 2 \mu_w \frac{d_o P_o}{\tau_o} \int_0^{\theta_o} \frac{e^{\mu_w(\theta - \theta_o)} \sin \theta}{1 + (v/c) \sin \theta} d\theta, \quad (28)$$

provided that P_o is greater than the critical pressure P_c of (25). Actually P_o must be much larger than P_c for (28) to be strictly valid. According to (28) and (25), the ratio P_o/P_c is of order h/d_o , and d_o/h has been assumed small throughout the analysis. That is why P_o rather than $(P_o - P_c)$ appears in (28), which otherwise is compatible with the empirical formula (1) implicit in the work of Zelenin, Vesselov, and Koniashin.

Apparently (28) cannot be evaluated in terms of elementary functions, but elementary forms are available for the important limits $v/c \rightarrow 0$ and $v/c \rightarrow \infty$. Thus as $v/c \rightarrow 0$,

$$h \rightarrow \frac{2\mu_w}{1 + \mu_w^2} \frac{d_o P_o}{\tau_o} (\mu_w \sin \theta_o - \cos \theta_o + e^{-\mu_w \theta_o}), \quad (29)$$

and in the opposite limit $v/c \rightarrow \infty$,

$$h \rightarrow \frac{2kd_o P_o}{\mu_r g v} (1 - e^{-\mu_w \theta_o}). \quad (30)$$

The intrinsic speed c has been eliminated from (30) by means of definition (22) to show that slot depth ceases to depend on shear strength at high feed rates. Notice that neither (29) nor (30) reaches a maximum under normal impingement, $\theta_o = \pi/2$ radians. The optimum angle of impingement depends on μ_w and v/c but always lies between $\pi/2$ and π .

7. Comparison with Experiment

Equation (28) is truly predictive, because all the parameters on the right-hand side can be measured prior to a rock-cutting experiment. The four material properties entering the definition of c are measurable by conventional means. Only μ_w is novel, and μ_w could be found by measuring the drag of a rough cavitating surface in a pressurized water tunnel, and reducing the data in terms of equation (14). Perhaps μ_w should be adjusted to absorb the discrepancy between the square jet assumed in the theory and the round jets used in practice, but μ_w is nearly universal and can be measured once and for all.

An experimental program is being formulated to test the predictions of (28). Meanwhile Olsen and Thomas have performed experiments to establish the plausibility of (28), in the absence of independent means to measure μ_w and some of the ingredients of c .

The operating conditions for the water jet were as follows:

$$\begin{aligned}d_o &= 0.030 \text{ inch,} \\ P_o &= 17,000 \text{ psi,} \\ \theta_o &= 90^\circ, \\ v &= 1 \text{ to } 400 \text{ in/sec.}\end{aligned}$$

The nozzle consisted of a 45° conical contraction followed by a 0.060 inch straight section of diameter 0.030 inch, not a particularly good geometry according to [3]. Feed rates below 10 in/sec were accomplished by a single rectilinear pass. The target rock was spun on a turntable for higher feed rates. The number of revolutions was chosen so that the accumulated depth of cut was about 0.5 inch, deep enough for accurate measurement. The nozzle exit was located within 0.5 inch of the target to minimize breakup of the jet stream.

The target was Wilkeson sandstone, quarried in Western Washington State. The properties of the sandstone are taken to be as follows:

$$\begin{aligned}\mu_r &= 1.0, \\ \tau_o &= 1000 \text{ psi,} \\ g &= 0.005 \text{ inch,} \\ k &= 8.6 \times 10^{-5} (\text{in/sec})/(\text{psi/in}), \\ c &= 17.2 \text{ in/sec.}\end{aligned}$$

The properties of Wilkeson sandstone have been determined only partly by independent measurement. The estimate $\mu_r = 1.0$ has been inferred from [10], page 178, and seems to be a reasonable average for rocks. The shear strength τ_0 has been deduced from a compression test, in which a cubic-inch sample failed at 4500 psi. Jaeger and Cook [10] show that the failure criterion (18) implies a ratio of compressive to shear strength equal to

$$2[(\mu_r^2 + 1)^{1/2} + \mu_r] ,$$

which equals 4.8 when μ_r is unity. Thus $\tau_0 \approx 1000$ psi, a reasonable value for a moderately soft sandstone. The grain diameter g was measured very roughly by micrometer. The estimate for the permeability k of Wilkeson sandstone is the result of unabashed curve fitting. No means were available to measure k independently during the first crude experiments, so the value 8.6×10^{-5} (in/sec)/(psi/in) was determined by fitting the asymptotic expression (30) to the values of h measured at high v .

It is worth saying a few words about k at this stage, because permeability will play the major role in the economics of hydraulic rock cutting. k depends on the viscous drag of fluid squeezing through the interstices between grains. The viscosity of the fluid can be eliminated through the formula

$$k = k'/\eta ,$$

where k' depends on the rock alone and has the dimensions of an area. To some extent the grain structure can be eliminated as well:

$$k = k^*g^2/\eta , \quad (31)$$

where k^* is dimensionless. Equation (31) conveys the useful implication that slot depth at high v is directly proportional to grain diameter g , rather than inversely proportional as (30) suggests. The length relevant to permeability is the gap between grains rather than their diameter, however, so k^* must be very small. Under the present assumptions about Wilkeson sandstone, for example, $k^* = 6.5 \times 10^{-7}$. The permeability k thus depends upon imperfections in grain alignment. Like electrical conductivity, also dependent upon imperfections, k varies over an enormous range, by a factor of 10^5 among rocks according to Table 2.2 of [11]. In that table the permeability of "sandstone" is given as 0.2 to

3.9×10^{-5} (in/sec)/(psi/in) in the present units, so the value 8.6×10^{-5} (in/sec)/(psi/in) would appear somewhat high. On the other hand, Jaeger and Cook cite a value 230×10^{-5} (in/sec)/(psi/in) for "Berea sandstone" on page 197 of [10]. The textbook values of k span too wide a range to help determine the permeability of Wilkeson sandstone, but the assumed value falls within the range and is not unreasonable.

Figure 7 is a comparison between the theory and Olsen and Thomas's data. The ordinate represents h and the abscissa v , both coordinates being logarithmic. The curve was obtained from equation (28) by numerical integration for the given experimental conditions and assumed material properties, and for

$$\mu_w = 0.42 \quad . \quad (32)$$

Agreement between experiment and theory is seen to be excellent. The measured values of h do appear to become constant at low v in accord with (29), and in the opposite extreme they decrease inversely with v in accord with (30). The theory accurately describes the shape of the transition between the two asymptotes. The choice $\mu_w = 0.42$ befitting the data, moreover, falls in the midst of the plausible range (15). The comparison in Fig. 7 is highly encouraging, though positive confirmation of the theory must await an independent measurement of k .

Olsen and Thomas also subjected Wilkeson sandstone to a few pressures P_o lower than 17,000 psi over a very limited range of feed rates. Figure 8 shows a sample of the results, for $d_o = 0.030$ inch and $\theta_o = 90^\circ$ as before. The depth h is plotted as a function of P_o for a feed rate $v = 40$ in/sec. The four experimental points were obtained by interpolating between data at nearby values of v , and the straight solid line follows from (28). The data describe an S-shaped curve, which tends toward the theory at high P_o . The fact that the first two points fall well below theory should come as no surprise, because equation (25) predicts a critical pressure $P_c = 7900$ psi when $v = 40$ in/sec. Notice that if h were assumed proportional to $(P_o - P_c)$ as shown by the dotted line, then the best choice for P_c would be only 4000 psi. The P_c of (25) should be interpreted as the pressure for which h falls short of theory by about half, rather than as an absolute cutoff.

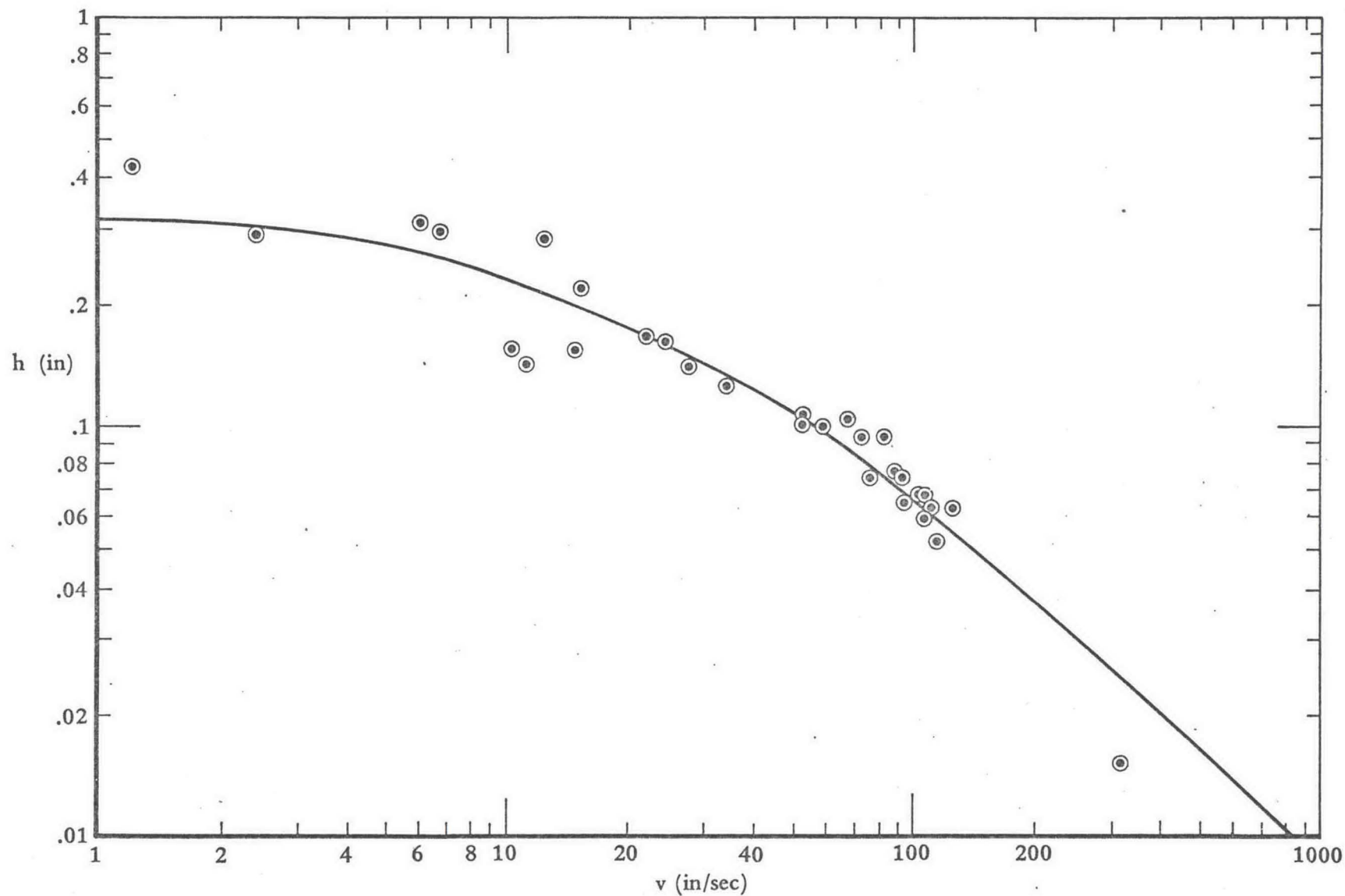


Figure 7. Comparison between experiment and theory for Wilkeson sandstone. The jet impinges normally with a diameter 0.030 inch and a total pressure 17,000 psi. The curve follows from (28) under appropriate assumptions about the parameters.

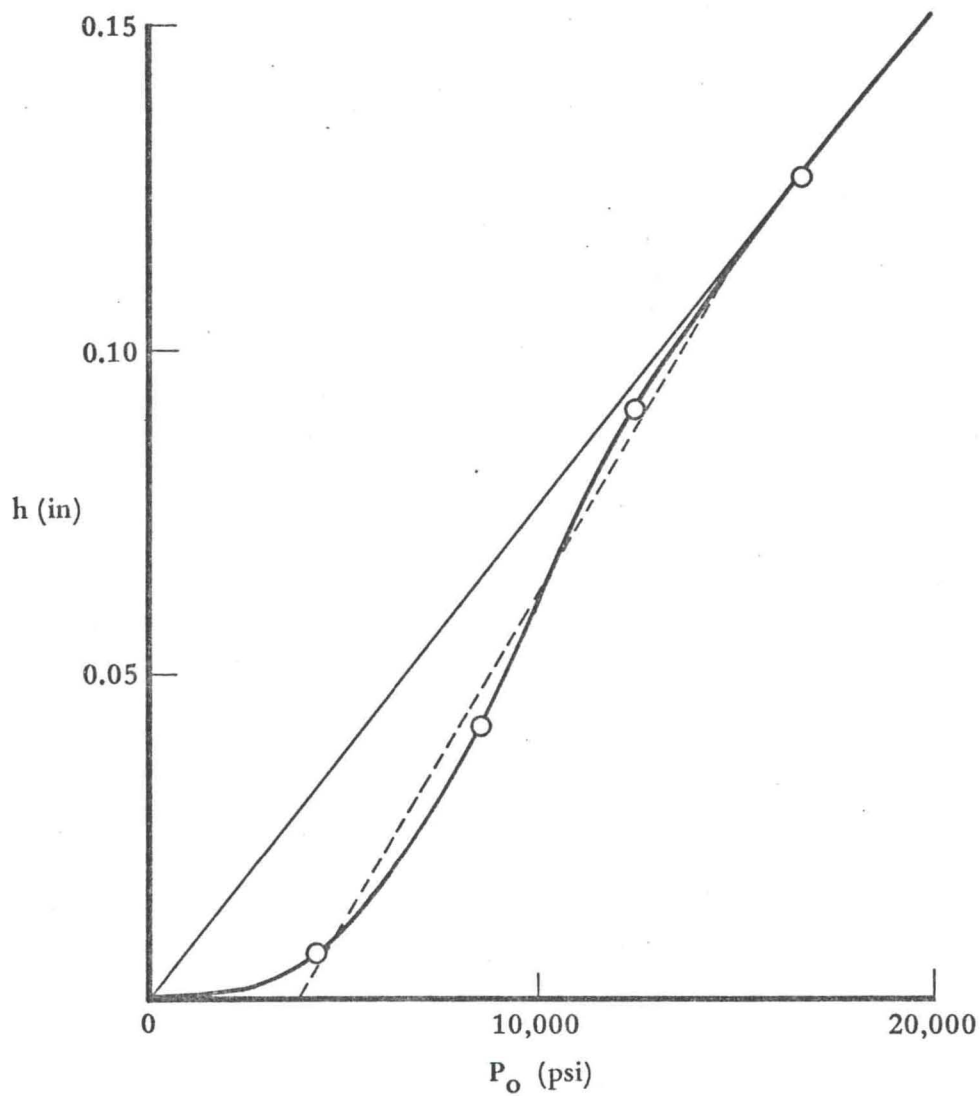


Figure 8. Variation of slot depth with jet pressure for Wilkeson sandstone at a feed rate $v = 40$ in/sec.

8. Practical Consequences

The theory implies some optimum strategies for hydraulic rock cutting, and they will serve as an appropriate conclusion.

Suppose the requirement is to make the deepest possible cut with a single pass of a water jet. The feed rate should be low according to (28) but not necessarily infinitesimal. The depth is sufficiently close to the asymptotic maximum (29) when v is perhaps one-third c . For a coefficient of Coulomb friction $\mu_w = 0.42$, the bracketed term in (29) reaches a softly defined maximum at an impingement angle $\theta_o = 150^\circ$. The conditions for maximum penetration can be summarized as follows:

$$\left. \begin{aligned} 0 < v &\lesssim (1/3)c , \\ \theta_o &= 150^\circ , \\ h_{\max} &= 1.01 \frac{d_o P_o}{\tau_o} . \end{aligned} \right\} \quad (33)$$

Under normal impingement, $\theta_o = 90^\circ$, the coefficient in the third member of (33) is 0.67, so the oblique impingement offers a 50% improvement in slot depth. In machinist's terminology, the jet should be set at a high positive rake, which forces it to swing through a large angle and cut deep. Note that shear strength τ_o is the only material property regulating h_{\max} .

It is possible to imagine situations in which h would be important, but usually multiple passes would permit cuts of any depth. When multiple passes are feasible, then the quantity of most importance is hv , the slot area created per unit time. It pays to raise the feed rate v as long as hv increases, because any degradation of h can be made up by multiple passes. According to (28), the rate of area creation hv rises monotonically with v toward the asymptote implicit in (30). For practical purposes v need not be more than four times c and must not be so large that the critical pressure P_c of (25) exceeds P_o . For $\mu_w = 0.42$, the conditions that maximize the rate of slot-area creation are as follows:

$$\left. \begin{aligned} (4)c &\lesssim v \lesssim (0.42 P_o / \tau_o - 1)c , \\ \theta_o &\rightarrow 180^\circ , \\ (hv)_{\max} &= 1.47 \frac{kd_o P_o}{\mu_r g} . \end{aligned} \right\} \quad (34)$$

Under normal impingement the coefficient in the third member of (34) is 0.97, so oblique impingement secures a 51% advantage in principle. The theoretical optimum requires that the jet be raked parallel to the rock surface, however, so that the flow swings a full 180° down through the cut. In practice the lip of rock above the impingement point would break away as $\theta_o \rightarrow 180^\circ$, but the greatest possible rake should be used short of gross failure.

A remarkable consequence of (34) is that shear strength τ_o governs the feed-rate window within which efficient cutting can take place but has no effect on the rate at which slot area can be created. The limited permeability k of the rock imposes an absolute upper limit on the rate of area creation. Permeability controls the economics of hydraulic rock cutting. Since permeability varies over a range of five decades, there will be some rocks that are susceptible to hydraulic cutting, and there will be some rocks that are not.

But there may be an escape from the limitation of permeability. If the rock is completely saturated prior to cutting, then the air-water interface WD shown in Fig. 6 does not exist, and the arguments of Section 5 break down. The pressure gradient beneath the cutting surface would relax to a level of order $(p_s - p_a)/d_o$, and equation (21) could be replaced with

$$\tau = \tau_o + \frac{\mu_r g}{d_o} (p_s - p_a) \approx \tau_o \left(1 + \frac{\mu_r}{\mu_w} \frac{g}{d_o} \right),$$

where the second form follows approximately from (14) if g is much less than d_o . The cutting depth might then approximate the maximum (29) regardless of feed rate. Whether saturation offers practical relief from the limitations of permeability is a matter for future research.

9. References

- [1] Hustrulid W. A. and Fairhurst C. A theoretical and experimental study of the percussive drilling of rock. *Int. J. Rock Mech. Min. Sci.* 8, 311-356 (1971).
- [2] Farmer I. W. and Attewell P. B. Rock penetration by high velocity water jet. *Int. J. Rock Mech. Min. Sci.* 2, 135-153 (1965).
- [3] Leach, S. J. and Walker G. L. Some aspects of rock cutting by high-speed water jets. *Phil. Trans. R. Soc.* A260, 295-308 (1966).
- [4] Brook N. and Summers D. A. The penetration of rock by high-speed water jets. *Int. J. Rock Mech. Min. Sci.* 6, 249-258 (1969).
- [5] Powell J. H. and Simpson S. P. Theoretical study of the mechanical effects of water jets impinging on a semi-infinite elastic solid. *Int. J. Rock Mech. Min. Sci.* 6, 553-564 (1969).
- [6] Zelenin A. N., Vesselov G. M. and Koniashin Y. G. Rock breaking with jet-stream under pressure up to 2,000 atm. Problems of Mining, Turpigorev Volume, 112-122, Moscow (1958). Translated by C. A. Procopov, Spokane Office of Mineral Resources and Spokane Office of Mining Research, U. S. Bureau of Mines, Spokane, Washington.
- [7] Contractor D. M. Application of fluid transients to hydraulic mining. ASME Paper No. 71-WA/FE-16 (1971).
- [8] Birkhoff G. and Zarantonello E. H. Jets, Wakes and Cavities, pp. 228-229, Academic Press, New York (1957).
- [9] Batchelor G. K. An Introduction to Fluid Dynamics, pp. 502-506, Cambridge University Press (1967).
- [10] Jaeger J. C. and Cook N. G. W. Fundamentals of Rock Mechanics, Methuen, London (1969).
- [11] Peck R. P., Hanson W. E. and Thornburn T. H. Foundation Engineering, John Wiley, New York (1953).